Role of Hydroxyl Side Chains in *Bombyx mori* Silk Sericin in Stabilizing Its Solid Structure

Hidetoshi Teramoto,[†,‡] Aya Kakazu,[‡] Kazuo Yamauchi,[‡] and Tetsuo Asakura*[,‡]

Division of Insect Sciences, National Institute of Agrobiological Sciences, Tsukuba, Ibaraki 305-8634, Japan, and Department of Biotechnology, Tokyo University of Agriculture and Technology, Koganei, Tokyo 184-8588, Japan

Received November 11, 2006; Revised Manuscript Received December 12, 2006

ABSTRACT: It is important to study the hydrogen-bonding character in hydrophilic polymers in detail to create new hydrophilic synthetic polymers controlled by hydration. In this paper, the role of hydroxyl side chains in sericin, a gluelike hydrophilic protein of *Bombyx mori* cocoon, in forming stable β-sheet aggregates is studied on the basis of ^{13}C solid-state NMR analyses. To clarify the molecular mechanism to stabilize the solid structure of sericin, ^{13}C CP/MAS and DD/MAS NMR measurements of native sericin and a model peptide of its crystal domain were performed at hydrated state. There are hydroxyl side chains of Ser and Thr residues in β-sheet structure which remain rigid after hydration. These hydroxyl side chains were assumed to clump adjacent β-sheets by hydrogen bonding at their OH groups. We inferred that Ser and Thr linkage sequences in the crystal domain are responsible for forming β-sheet aggregates and generating the structural stability of sericin.

Introduction

Hydrophilic polymeric materials, both naturally derived and synthetic, have been intensely studied as biomedical materials because of their good biocompatibility.[1] The hydrogen-bonding ability of polar functional groups in hydrophilic polymers is one of the important features to characterize the properties of these materials. Hydroxyl groups often play an important role in the structural formation of polymers such as silk, cellulose, or poly(vinyl alcohol) (PVA) through the formation of intra- and intermolecular hydrogen bonds. In the silk fiber of *Bombyx mori* (domesticated silkworm),[2] the contribution of Ser hydroxyl groups to the intermolecular hydrogen-bonding network among silk fibroin molecules has been suggested by solid-state NMR analyses.[3−5] Sericin, a gluelike protein of *Bombyx mori* silk,[6,7] exhibits high hydrophilicity due to its high content of hydrophilic amino acids including Ser (ca. 35%) and Thr (ca. 10%).[8,9] Abundant hydroxyl groups in sericin are expected to play a crucial role in its structural formation.

Sericin is synthesized exclusively in the middle silk glands of *Bombyx mori* larvae and stored as an aqueous solution until spinning. Sericin glues fibroin threads together in *Bombyx mori* cocoon and fills the gaps of fibrous framework to increase the toughness of the cocoon. Once sericin is secreted and transformed into solid state, it exhibits low solubility in water at ambient temperature despite its high content of hydrophilic amino acids. Therefore, there must be some molecular mechanisms to stabilize the solid structure of sericin achieved by its characteristic primary structure. However, detailed molecular mechanisms behind the structural formation of sericin at native state have not been investigated because of its vulnerability to heat or alkaline treatment required to separate it from fibroin threads. In order to avoid the problem in sericin degradation, a new silkworm strain named Sericin Hope was developed.[10] Sericin Hope secretes almost exclusively sericin (ca. 98%), which enables us to obtain native sericin because the separation process from fibroin threads is not required. We have investigated the characteristics of native sericin derived from Sericin Hope such as structural transition during spinning,[11,12] molecular orientation behavior,[13] or degradation pattern[11] using FTIR and NMR spectroscopies.

Recently, sericin is anticipated as a novel naturally derived biomaterial due to its distinct characteristics,[14] such as affinity to human skin and hair,[15] induction of heterogeneous nucleation of apatite,[16,17] and enhanced attachment of primary cultured human skin fibroblasts.[18] In addition, native sericin without degradation exhibits improved mechanical strength, which will expand the possibilities of sericin as a material. Therefore, the structure−function relationships of native sericin, especially the role of the hydroxyl groups in its structural formation, are of great interest in connection with its physiological functions and application as a material.

X-ray and solid-state NMR analyses have been generally used to investigate the structure of solid polymers at a molecular level. However, X-ray analysis is not efficient for sericin because of its low crystallinity. Therefore, solid-state NMR would be a suitable means for the structural analysis of sericin because information from both crystalline and amorphous regions can be equally obtained. Moreover, dynamic properties can be investigated by solid-state NMR using varied measurement techniques.

In this study, we applied ^{13}C solid-state NMR spectroscopy to clarify the molecular mechanism behind the stabilization of the solid structure of sericin. We considered that amino acid residues in sericin engaged in structural stabilization would form rigid and hydrophobic domains which are not easily hydrated. We thus applied ^{13}C cross-polarization/magic angle spinning (CP/MAS) and single-pulse, dipolar decoupled/magic angle spinning (DD/MAS) NMR measurements to hydrated sericin samples in order to clarify amino acid residues leading to rigid and mobile domains at hydrated state. A model peptide designed from the repetitive region of sericin was investigated to clarify amino acid sequences acting as a motif to stabilize the solid structure of sericin. Detailed NMR analyses suggested that Ser and Thr linkages found in the repetitive region are probable

* Corresponding author. E-mail: asakura@cc.tuat.ac.jp.
[†] National Institute of Agrobiological Sciences.
[‡] Tokyo University of Agriculture and Technology.

10.1021/ma062604e CCC: $37.00
Published on Web 01/19/2007

candidates as sequences generating the structural stability of sericin.

Experimental Section

Sample Preparations. The larvae of Sericin Hope silkworm were reared on artificial diet (Nihon Nosan Co., Yokohama, Japan). Their cocoon shells were collected and directly used for spectroscopic analyses as native sericin. Sericin with higher β-sheet content was prepared by immersing Sericin Hope cocoon shell in excess formic acid for 2 h at 25 °C followed by air-drying. A sericin model peptide which consists of 38 amino acids, SVSSTGSSSNTDSNSNSAGSSTSGGSSTYGYSSNSRDG, and its ^{13}C-labeled one, SVSST[1-^{13}C]G^{6}SSSNTDSNSNS[3-^{13}C]A^{18}GSSTSG[2-^{13}C]G^{25}SSTYGYSSNSRDG, were synthesized by solid-phase Fmoc chemistry on a fully automated Pioneer Peptide Synthesis System (Applied Biosystems Ltd., Warrington, UK). The synthesized peptides were dissolved in 9 M LiBr aqueous solution, dialyzed against deionized water, and lyophilized. Hydrated samples were prepared by immersing each sample in excess Milli-Q water over 24 h at 25 °C.

Spectroscopic Measurements. The ^{13}C solid-state NMR spectra were recorded at 25 °C using a CMX Infinity 400 NMR spectrometer (Chemagnetics Inc., Fort Collins, CO) operating at 100.04 MHz for the ^{13}C nucleus. Successive CP/MAS and DD/MAS experiments were performed for hydrated samples. Each sample was packed in a 4 mm diameter zirconia rotor and spun at 9 kHz. For hydrated samples, a sample rotor was sealed with epoxy resin to prevent evaporation of water during measurements. The spectral width, acquisition time, and repetition time for CP/MAS and DD/MAS experiments were 35 kHz, 14.6 ms, and 3 s, respectively. The contact time of 2 ms and TPPM decoupling were employed for CP/MAS experiments. The 90° pulses for carbon and proton were 3.25 μs. The dipolar decoupling field strength was 77 kHz. The number of acquisitions was 16 384. The ^{13}C chemical shifts were calibrated indirectly through the adamantane methine peak observed at 28.8 ppm relative to tetramethylsilane at 0 ppm.

FTIR spectra were collected using a Herschel FT/IR-350 spectrometer (Jasco Inc., Tokyo, Japan) at a resolution of 4 cm^{-1}. All samples and backgrounds were scanned 64 times. Attenuated total reflection (ATR) measurements were performed using a DuraSampl*IR* II single-reflection ATR attachment (SensIR Technologies, Danbury, CT).

Results and Discussion

Analysis of Native Sericin. ^{13}C CP/MAS and DD/MAS experiments were employed to enhance signals from rigid and mobile environments, respectively. Figure 1 shows (a) the ^{13}C CP/MAS NMR spectrum of the native cocoon shell from Sericin Hope silkworm (termed native sericin) at dry state, (b) ^{13}C CP/MAS and (c) ^{13}C DD/MAS NMR spectra of the native sericin at hydrated state, and (d) the ^{13}C solution NMR spectrum of the regenerated sericin in aqueous solution. Table 1 summarizes the chemical shifts of the carbonyl, Ser Cα, and Ser Cβ peaks of the native sericin before and after hydration. The assignments have been reported previously.[11] For a comparison, ^{13}C NMR chemical shifts of the regenerated sericin solution[11] and liquid silk[19] as references of random coil structure and silk fiber[19] as a reference of β-sheet structure were shown together.

Much improved spectral resolution was observed in both CP/MAS and DD/MAS spectra by hydration (Figure 1b,c) as compared with a broad feature of the CP/MAS spectrum of the native sericin at dry state (Figure 1a). This is due to either hydration-induced change in molecular motion or conformation. Similar resolution enhancements in ^{13}C solid-state NMR spectra by hydration have already been reported for hydrophilic polymers such as spider silk,[23,24] collagen,[25,26] and PVA.[27] The DD/MAS spectrum of the native sericin after hydration (Figure 1c) exhibited a quite similar spectral pattern to the spectrum of the regenerated sericin solution reported previously[11] (Figure 1d). Sericin takes largely random coil structure in solution.[11] Hence, the similar spectral pattern to the solution shows that the DD/MAS spectrum enhances carbons in mobile domains, forming solution-like random coil structure. The CP/MAS spectrum, on the other hand, enhances signals from carbons in rigid environments. The apparent difference between the CP/MAS and DD/MAS spectra showed that the native sericin contains domains which exhibit largely different dynamic properties at hydrated state.

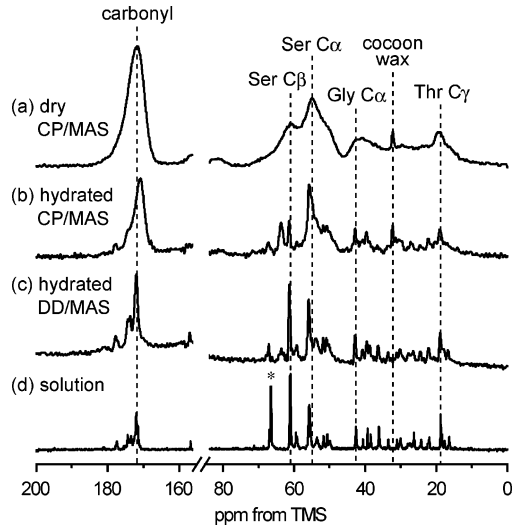

Figure 1. (a−c) ^{13}C solid-state NMR spectra of the cocoon shells of Sericin Hope silkworm (native sericin): (a) the CP/MAS spectrum at dry state and (b, c) the CP/MAS and DD/MAS spectra at hydrated state, respectively. (d) The solution spectrum of the regenerated sericin solution[11] shown as a reference. The peak marked with an asterisk is from 1,4-dioxane added as an internal standard. The sharp peak at 32.2 ppm observed in the CP/MAS NMR spectra is assignable to the main methylene peaks of cocoon wax[20] because its chemical shift is in agreement with that of *n*-alkanes[21] and natural beeswax.[22]

In the carbonyl region, the C═O main peak was observed at 171.7 ppm at dry state. Although a number of peaks arising from different amino acids are overlapped in this region, Ser C═O probably has a major contribution because of its abundance (ca. 35%) in sericin. After hydration, the CP/MAS and DD/MAS experiments gave their C═O main peaks at 170.8 and 172.0 ppm, reflecting rigid and mobile domains, respectively. The peak at 172.0 ppm in the DD/MAS experiment was assigned to random coil structure by the comparison with the sericin solution. The DD/MAS experiment detected mobile domains where carbonyl carbons were highly hydrated to form random coil structure. The peak at 170.8 ppm in the CP/MAS experiment was assigned to the β-sheet structure with reference to the data from a variety of polypeptides.[28]

Figure 2 shows the expanded spectra of the high-field region (35−75 ppm) of Figure 1. All peaks clearly seen in the DD/MAS spectrum were assigned on the basis of the assignment in the sericin solution. The chemical shifts of each peak in the DD/MAS spectrum arose from mobile carbons involved in random coil structure. The Asp Cβ and Asn Cβ peaks were suppressed in the CP/MAS experiment. These suppressed peaks showed that the side-chain mobility of these residues increased by hydration. On the other hand, apparent peak suppression in the DD/MAS experiment occurs for two peaks at 63.7 and 55.1 ppm. We attributed the peak at 63.7 ppm to the Cβ of the Ser residues in β-sheet structure with reference to the data of silk fiber (Table 1). This assignment has been confirmed by selective ^{13}C enrichment experiment at Ser Cβ (unpublished data). Then,

Table 1. ^{13}C NMR Chemical Shifts (in ppm from TMS) of the Native Sericin, the FA-treated Sericin, and the Sericin Model Peptide at Dry and Hydrated States

	native sericin		FA-treated sericin		sericin model peptide				
residue	dry	hydrated	dry	hydrated	dry	hydrated	sericin solution[11]	liquid silk[19]	silk fiber[19]
C═O[a]	171.7	170.8	170.9	170.9	171.0	170.0	171.5 (Gly)	171.3 (Gly)	169.3 (Gly)
		172.0		172.0		171.7	172.0 (Ser)	172.4 (Ser)	*b*
Ser Cα	55.0	55.1	54.7	55.0	55.1	54.9	55.7	55.9	54.6
		55.9		55.9		55.7			
Ser Cβ	60.9	61.3	63.0	61.3	60.8	61.2	61.0	61.3	63.9
		63.7		63.6		63.5			

[a] Chemical shifts of the main peaks were shown except for the reference data. [b] Ser C═O was overlapped with Ala C═O at 172.2 ppm.

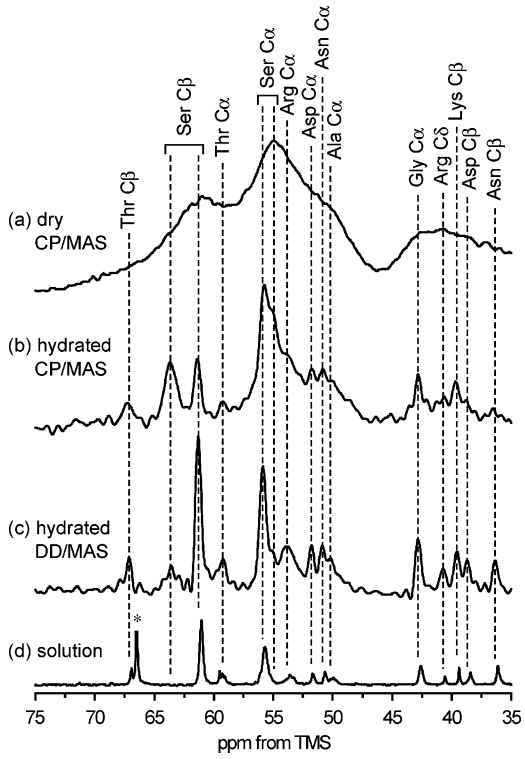

Figure 2. (a−c) ^{13}C solid-state NMR spectra of the native sericin: (a) the CP/MAS spectrum at dry state and (b, c) the CP/MAS and DD/MAS spectra at hydrated state, respectively. (d) The solution spectrum of the regenerated sericin solution[11] shown as a reference. The peak marked with an asterisk is from 1,4-dioxane added as an internal standard.

we assigned the other peak at 55.1 ppm to the Cα of the Ser residues in β-sheet structure.

The peak suppression in the DD/MAS experiment observed with the β-sheet component of Ser Cβ at 63.7 ppm revealed that the side chains of the Ser residues in β-sheet structure were located in rigid and hydrophobic environments. The observed rigidity of the Ser side chains in β-sheet conformation is attributable to the formation of hydrogen bonding at their OH groups. Within a β-sheet, side chains point alternatively above and below the sheet and are capable of interacting with neighboring sheets. Hence, we speculated that the OH groups of the Ser residues on β-sheets form hydrogen bonds with the C═O groups of the main chains or the OH groups of the side chains on the neighboring sheets to induce the aggregation of the β-sheets.

Involvement of Ser side chains in interchain hydrogen bonding was previously investigated with *Bombyx mori* silk fibroin using solid-state NMR spectroscopy.[3−5] Kameda and colleagues suggested that the rigid fraction of Ser side chains detected by ^{2}H solid-state NMR forms interchain hydrogen bonding.[3] Yao and colleagues revealed the ability of Ser residues to stabilize the extended structure by intermolecular hydrogen bonding using ^{13}C solid-state NMR.[4] White and Wang performed 2D solid-state ^{1}H−^{13}C HETCOR experiments of *Bombyx mori* and *Samia cynthia ricini* silk fibroins and revealed that the Ser side chains in *Bombyx mori* fibroin exhibited much stronger correlation.[5] They concluded that Ser residues exist in a more rigid or constrained environment, suggesting the involvement of Ser side chains in interchain hydrogen bonding. In addition, involvement of intermolecular hydrogen bonding in hydrogel formation of PVA was previously investigated using ^{13}C solid-state NMR.[29−31] Similarly to our observations in this study, signals from rigid carbons of PVA in the gel state were selectively observed by ^{13}C CP/MAS measurements, which has been assigned to the carbons connected to the OH groups involved in the formation of intra- and intermolecular hydrogen bonds. In particular, intermolecular hydrogen bonding was found to play an important role in the formation of PVA hydrogel through the formation of cross-linkings between polymer chains.[30] From these previous investigations, it would be quite reasonable to assume that the OH groups of Ser residues in sericin form intermolecular hydrogen bonds along with *Bombyx mori* silk fibroin and PVA to construct network structure.

Analysis of Sericin with Higher β-Sheet Content. The β-sheet formation and its aggregation is probably the key process to stabilize the solid structure of sericin. The ^{13}C solid-state NMR analysis of the native sericin implies the involvement of the Ser side chains in clumping the β-sheets by hydrogen bonding. In order to confirm this assumption, the effect of the β-sheet formation on the hydrated structure of sericin was then investigated. It has been reported that the formic acid treatment of silk fibroin increases its β-sheet content.[4,32] Therefore, formic acid treatment was also applied to silk sericin to increase its β-sheet content. Figure 3A shows the ^{13}C CP/MAS spectra of (a) the native sericin and (b) the formic acid-treated sericin (termed FA-treated sericin). The Ser Cβ peak is shifted to lower field from 60.9 to 63.0 ppm by the treatment, and the carbonyl and Ser Cα peaks are slightly shifted to higher field from 171.7 to 170.9 ppm and 55.0 to 54.7 ppm, respectively. These peak shifts are consistent with the general behavior observed in transition from disordered to β-sheet structures in view of the ^{13}C chemical shifts of the Ser Cα and Ser Cβ carbon signals listed in Table 1. Figure 3B represents the ATR-FTIR spectra of (a) the native sericin and (b) the FA-treated sericin. The amide I region around 1700−1600 cm^{-1} is shown because of its sensitivity to protein secondary structure. The spectrum before the formic acid treatment exhibited its peak top at 1641 cm^{-1} with a shoulder peak at 1619 cm^{-1}. These absorptions are typical of random coil structure and aggregated strands, respectively.[13,33] The absorption of the aggregated strands at 1619 cm^{-1} was remarkably increased by the formic acid treatment. From these analyses, it was confirmed that the FA-treated sericin contains larger amount of the β-sheet aggregates than the native sericin.

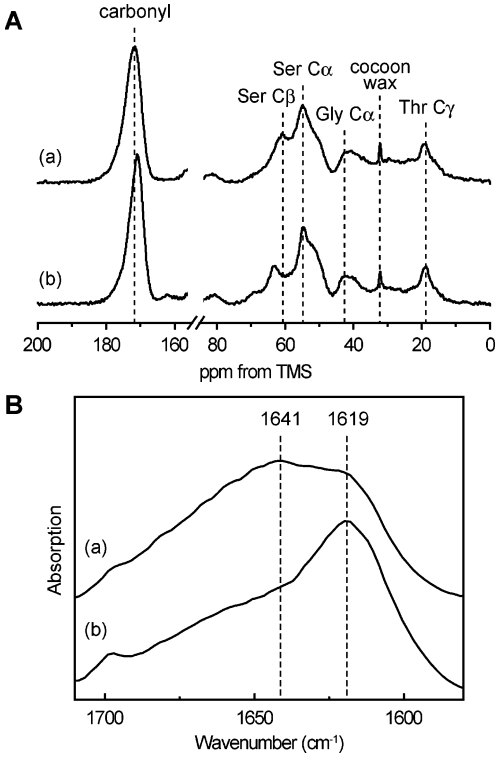

Figure 3. (A) ^{13}C CP/MAS NMR and (B) ATR-FTIR spectra of (a) the native sericin and (b) the FA-treated sericin. Baseline correction around the amide I region was performed in the ATR-FTIR spectra.

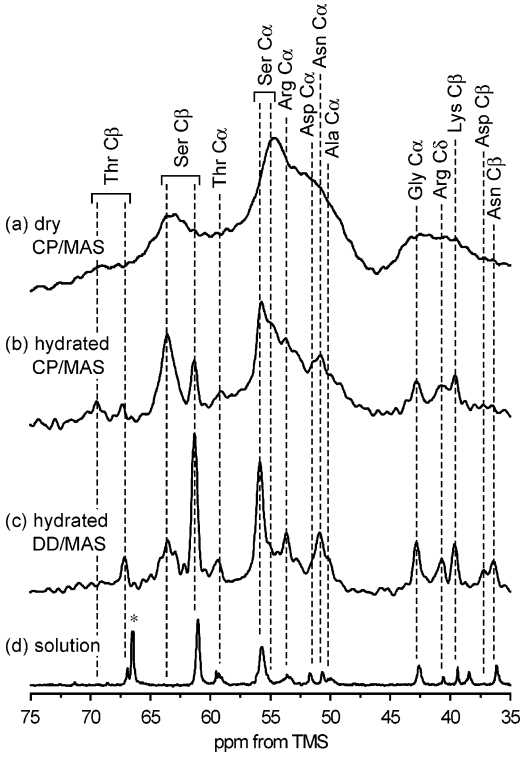

Figure 4. (a−c) ^{13}C solid-state NMR spectra of the cocoon shells of Sericin Hope silkworm treated with formic acid (FA-treated sericin): (a) the CP/MAS spectrum at dry state and (b, c) the CP/MAS and DD/MAS spectra at hydrated state, respectively. (d) The solution spectrum of the regenerated sericin solution[11] shown as a reference. The peak marked with an asterisk is from 1,4-dioxane added as an internal standard.

Figure 4 shows the high-field region (35−75 ppm) of (a) the ^{13}C CP/MAS NMR spectrum of the FA-treated sericin at dry state, (b) ^{13}C CP/MAS and (c) ^{13}C DD/MAS NMR spectra of the same sample at hydrated state, and (d) the ^{13}C solution NMR spectrum of the regenerated sericin solution. The chemical shifts of the carbonyls, Ser Cα, and Ser Cβ peaks of the FA-treated sericin before and after hydration are summarized in Table 1. The DD/MAS spectrum at hydrated state (Figure 4c) exhibited almost the same spectral feature with that before formic acid treatment (Figure 2c), except for the peak positions of Asp Cα and Cβ, which are shifted to higher field due to protonation. The Asp Cβ and Asn Cβ peaks were suppressed in the CP/MAS experiment similarly to the native sericin, showing that these residues were located in hydrophilic regions which were not affected by the formic acid treatment. In the CP/MAS spectrum at hydrated state (Figure 4b), the relative intensity of the β-sheet component of Ser Cβ at 63.6 ppm to the disordered component at 61.3 ppm apparently increased compared with the native sericin (Figure 2b). It is strongly suggested that the observed increase of the β-sheet component of Ser Cβ is correlated with the aggregation of the β-sheets, combined with the data of FTIR analysis (Figure 3B). A small peak assignable to the β-sheet component of Thr Cβ appeared at 69.5 ppm in the CP/MAS spectrum at hydrated state (Figure 4b). This peak was suppressed in the DD/MAS experiment along with the β-sheet component of Ser Cβ, indicating that the hydroxyl side chains of the Thr residues in β-sheet conformation are involved in interaction among the β-sheets. The increase of the rigid side chains of Ser and Thr residues shows that the β-sheet aggregates are stable and not transformed to random coil structure by hydration. This observation is consistent with the previous results that iterative hydration and dehydration causes irreversible β-sheet formation in sericin film.[34]

Zhu and colleagues reported that the adhesive strength of sericin in cocoon becomes strong when cocoon production by silkworm is done at high temperature and humidity.[35] This phenomenon is considered to be due to the structural transition of sericin to β-sheet-rich structure induced by high temperature and humidity. It has been generally acknowledged that sericin with β-sheet-rich structure exhibits increased thermal stability along with decreased water solubility.[34,35] Our previous FTIR analysis revealed that the formation of intermolecular hydrogen bonding generate the molecular orientation of sericin upon stretching.[13] These observations suggest that the formation and aggregation of β-sheets by intermolecular hydrogen bonding of Ser and Thr side chains is deeply correlated with the material properties of sericin.

Improvement of material property by the formation of hydrogen-bonding network has been observed in synthetic polymer materials. Kobayashi and colleagues reported that relatively hard PVA hydrogel can be obtained with syndiotactic PVA because it sterically favors intermolecular hydrogen bonding compared with isotactic and atactic PVAs.[30] It was also reported that improvement of the compression performance of rigid-rod polymer fiber was achieved by introducing hydrogen-bonding network among the polymer chains.[36] These investigations strongly suggest that controlling hydrogen bonding in sericin is the key to improve the material properties of sericin materials.

Analysis of Sericin Model Peptide. The primary structure of sericin has been largely elucidated.[8,37,38] Therefore, it would be possible to attribute the observations in natural sericin to specific amino acid sequences. The native sericin consists of several protein components.[11,13] The most abundant one has the largest molecular weight over 250 kDa and probably corresponds to Ser1C protein encoded by *Ser1* gene.[8,37] A schematic structure of Ser1C is depicted in Figure 5. Most of Ser1C is

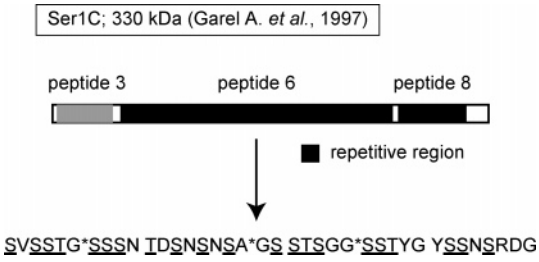

Figure 5. Schematic structure of Ser1C and primary sequence of a synthesized sericin model peptide derived from the peptide 6 encoded by the exon 6 of *Ser1* gene.[8] Ser and Thr residues in the model peptide are underlined. ^{13}C-labeled sites are marked with asterisks.

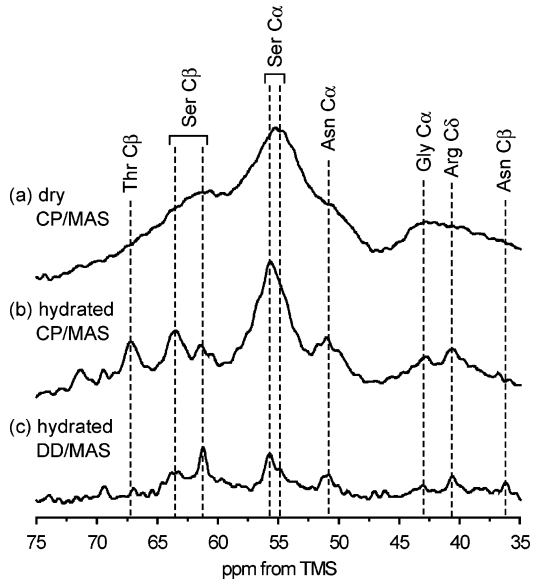

Figure 6. ^{13}C solid-state NMR spectra of the sericin model peptide derived from the Ser-rich repetitive region: (a) the CP/MAS spectrum at dry state and (b, c) the CP/MAS and DD/MAS spectra at hydrated state, respectively.

covered by the peptides 3, 6, and 8 encoded by the exons 3, 6, and 8 of Ser1C cDNA.[8] The peptides 6 and 8 contain about 70 repeats of a characteristic 38-amino acid repetitive motif rich in Ser (ca. 40%), whereas the peptide 3 serves as a hydrophilic region with high content of charged residues.[8] The repetitive sequence dominates a large part of Ser1C and characterizes sericin and has been predicted to have strong tendency to form β-sheet structure.[8,39] We synthesized a 38-amino acid peptide, SVSSTGSSSNTDSNSNSAGSSTSGGSSTYGYSSNSRDG, derived from the peptide 6 (Figure 5) to clarify its involvement in the β-sheet aggregation through Ser and Thr side chains.

Figure 6 shows (a) the ^{13}C CP/MAS NMR spectrum of the model peptide at dry state and (b) ^{13}C CP/MAS NMR and (c) ^{13}C DD/MAS NMR spectra of the same sample at hydrated state. The chemical shifts of the carbonyl, Ser Cα, and Ser Cβ peaks of the model peptide before and after hydration are summarized in Table 1. When the model peptide was hydrated, part of it (ca. 30 wt %) dissolved in water. The solubilized portion was removed by centrifugation, and the remaining precipitate was used for NMR measurements at hydrated state. Hence, Figure 6b,c shows the spectra of the insoluble portion of the peptide. The DD/MAS experiment at hydrated state gave relatively weak signals compared with the native sericin (Figure 2c), which indicates that the model peptide contains a relatively small amount of mobile domains. The FA-treated sericin exhibited intense peaks in the DD/MAS experiment at hydrated

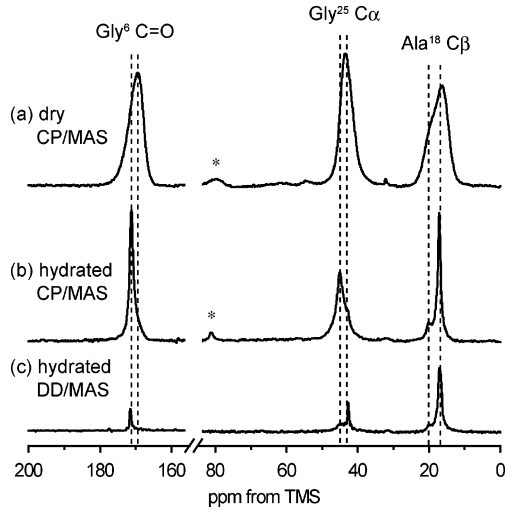

Figure 7. ^{13}C solid-state NMR spectra of the ^{13}C-labeled sericin model peptide: (a) the CP/MAS spectrum at dry state and (b, c) the CP/MAS and DD/MAS spectra at hydrated state, respectively. The signals from natural abundance ^{13}C nuclei were subtracted. Spinning sidebands are indicated by asterisks.

state in spite of its high β-sheet content. The peptide 3, which contains many charged residues, might be responsible for a significant part of hydrophilic regions in the native sericin. Ser Cβ exhibited two peaks at 63.5 and 61.2 ppm at hydrated state, which were assignable to β-sheet and random coil (disordered) structures, respectively. The β-sheet component at 63.5 ppm was suppressed in the DD/MAS experiment, whereas the random coil component at 61.2 ppm was suppressed in the CP/MAS experiment. Apparently, Ser Cβ in the model peptide exhibited the same behavior with the native sericin. This result supports a view that the Ser-rich repetitive sequence is mainly responsible for the β-sheet aggregations in the native sericin. The relative intensity of the β-sheet component of Ser Cβ was larger than that observed with the native sericin, which would reflect the high β-sheet forming property of the model peptide. The suppression of the Thr Cβ peak at 67.2 ppm in the DD/MAS experiment showed its rigidity at hydrated state although its chemical shift is in the range of disordered structure. The Asn Cβ peak was suppressed in the CP/MAS experiment similarly with the native sericin, indicating that the Asn residues are located in hydrophilic regions. From these analyses, we assumed that the sequences containing Ser and Thr linkages, SSTGSSS and SSTSGGSST, form the β-sheet aggregates clumped by multiple hydroxyl side chains and that the Asn-rich sequence, NTDSNSN, serves as a hydrophilic domain.

In order to obtain complementary structural information about the Ser and Thr linkages and the Asn-rich sequence in the model peptide, site-specific ^{13}C-labeling was performed at three sites: Gly^{6} C=O, Gly^{25} Cα, and Ala^{18} Cβ (Figure 5). Gly^{6} and Gly^{25} are located between the Ser and Thr linkages, and Ala^{18} is located near the Asn-rich sequence. Figure 7 shows (a) the ^{13}C CP/MAS NMR spectrum of the ^{13}C-labeled model peptide at dry state and (b) ^{13}C CP/MAS and (c) ^{13}C DD/MAS NMR spectra of the same sample at hydrated state. The chemical shifts of ^{13}C-labeled carbons are summarized in Table 2. For a comparison, the typical chemical shifts of random coil, α-helix, and β-sheet structures are shown together.

The three signals from ^{13}C-labeled carbons in the CP/MAS spectrum at dry state (Figure 7a) exhibited heterogeneous peak features, indicating that the structure of the model peptide was

Table 2. ^{13}C NMR Chemical Shifts (in ppm from TMS) of the ^{13}C-Labeled Carbons in the Sericin Model Peptide

residue	^{13}C-labeled site	dry	hydrated *a*	hydrated *b*	random coil[c]	α-helix[40]	β-sheet[28]
Gly C═O	Gly^{6}	169.5	171.2	171.5	171.3	172.3	169.1
Gly Cα	Gly^{25}	43.5	45.1	42.7	42.9	44.0	42.4
Ala Cβ	Ala^{18}	16.1[d]	17.1	17.1	16.6	15.7	19.6
		19.6[d]					22.2

[a] The chemical shifts of the major peaks in the CP/MAS experiment are shown. [b] The chemical shifts of the major peaks in the DD/MAS experiment are shown. [c] The random coil chemical shifts were obtained from the solution NMR.[28] [d] The chemical shifts of the fractions obtained by peak deconvolution are shown.

not homogeneous. The chemical shift of the Gly^{6} C═O peak (169.5 ppm), which is close to the typical value of β-sheet structure, suggests that Gly^{6} favors β-sheet conformation at dry state. The Gly^{25} Cα peak was observed at 43.5 ppm, which is between the typical values of random coil and α-helix structures. This result indicates that Gly^{25} forms disordered or α-helix conformations at dry state. The Ala^{18} Cβ peak exhibited its peak top at 16.3 ppm with an apparent shoulder peak around 20 ppm. The chemical shifts of the fractions were determined to be 16.1 and 19.6 ppm by peak deconvolution, which were assigned to disordered and β-sheet structures, respectively. This result shows that Ala^{18} forms disordered and β-sheet conformations at dry state. These spectral data showed that the model peptide contained a significant amount of disordered structure. The partial dissolution of the peptide in water might be due to the coexistence of the disordered-rich peptide molecules.

The CP/MAS spectrum after hydration free from soluble portion gave almost a single peak for each carbon, suggesting that the insoluble peptide portion takes largely a uniform structure when it is hydrated. The Gly^{6} C═O peak was observed at 171.2 ppm in the CP/MAS experiment after hydration. This chemical shift is in agreement with the typical value of random coil structure. In the DD/MAS experiment, Gly^{6} C═O gave a small peak at 171.5 ppm, which is also assignable to random coil structure. This result showed that hydration affected the local conformation of Gly^{6} and transformed it into almost completely disordered (random coil) structure. However, judging from the relatively intense signal from Gly^{6} C═O in the CP/MAS experiment, most of Gly^{6} C═O remained rigid despite that it formed disordered structure by hydration. We assume that the sequences, SST and SSS, neighboring Gly^{6} form a rigid environment through interchain interaction of their hydroxyl side chains and restrict the movement of Gly.^{6} Gly^{25} Cα gave a relatively broad peak at 45.1 ppm in the CP/MAS experiment at hydrated state. This chemical shift is not always in agreement with that of any typical conformation for Gly Cα but is closest to α-helix structure. This observed unusual chemical shift might be due to some structural distortion at Gly.^{25} In the DD/MAS experiment, Gly^{25} Cα gave only a small peak at 42.7 ppm assigned to random coil structure. The relatively intense signal in the CP/MAS experiment showed that most of Gly^{25} was located in a rigid environment along with Gly.^{6} We assume that the sequences, SSTS and SST, surrounding Gly^{25} interact with adjacent chains and yield structural distortion at Gly.^{25} The Gly Cα peak around 45 ppm was not clearly observed in the CP/MAS spectrum of the natural abundance model peptide (Figure 6b), indicating that the observed unusual chemical shift might be unique for Gly.^{25} The Ala^{18} Cβ peak was observed at 17.1 ppm in the CP/MAS experiment at hydrated state. This chemical shift is in the region of random coil structure. In the DD/MAS experiment, the Ala^{18} Cβ was observed at the same position, and its relatively large peak intensity is due to the fast rotation of Ala methyl groups. Only weak signals were observed at

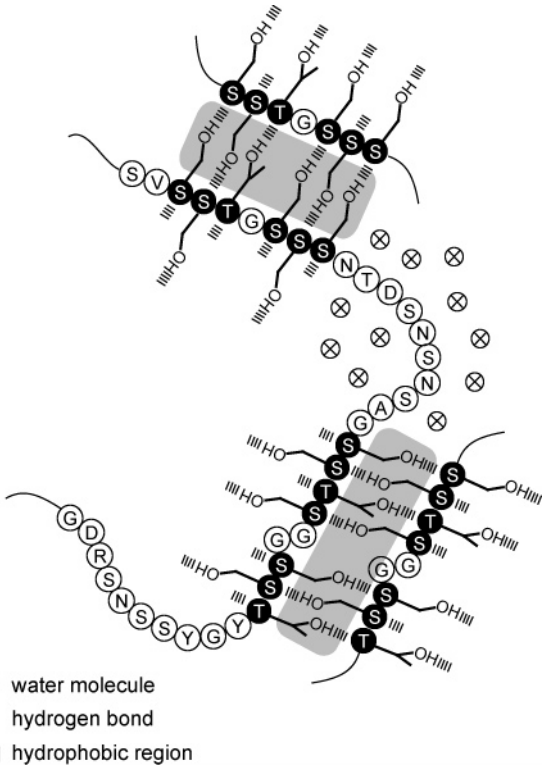

Figure 8. Schematic model of hydrated structure of sericin stabilized by the aggregation of the β-sheets. The Ser and Thr residues forming β-sheets are depicted as white character on a black background. Presumed hydrogen bonds between the OH groups of the Ser and Thr side chains and the C═O groups of the main chains on the adjacent sheets are emphasized. β-Sheet planes are perpendicular to the plane of the paper.

β-sheet position in both the CP/MAS and DD/MAS spectra, showing that hydration changed the β-sheet structure of Ala^{18} found at dry state to almost completely the random coil structure. We assume that Ala^{18} is located at a position which is easily hydrated due to the hydrophilicity of the neighboring Asn-rich sequence.

Presumed Molecular Mechanism in Structural Stabilization of Sericin. Figure 8 shows a schematic model of hydrated structure of sericin stabilized by the formation of the β-sheet aggregates. The Ser-rich 38-amino acid repetitive motif is described. The model structure was presumed from a series of ^{13}C solid-state NMR analyses. The Ser and Thr linkages and the Asn-rich sequence are supposed to take β-sheet and random coil structures at hydrated state, respectively, and form hydrophobic and hydrophilic regions. In the model, the hydroxyl side chains of Ser and Thr residues forming the β-sheets protrude from both side of the sheets and clump the neighboring sheets. Formation of hydrogen bonds between the OH groups of the side chains and the C═O groups of the main chains is assumed as a major factor to stabilize the β-sheet aggregates

because similar intermolecular hydrogen bonds between the OH groups of the Ser side chains and the C═O groups on the adjacent peptide chains in silk fiber have been suggested.[3,4] The aggregation of the β-sheets would make the regions among the sheets hydrophobic, which might prevent the access of water molecules. At dry state, sericin is considered to take a largely disordered structure. When sericin is hydrated, the formation of the β-sheet aggregates are supposed to be induced, which might prevent its dissolution in water. Peptide chains containing hydroxyl side chains in disordered structure will become mobile by hydration, which may transform into the more stable β-sheet aggregates. We infer that such kind of molecular mechanism might govern the dynamic behavior of sericin to water and generate its structural stability in cocoon.

Huang and colleagues[39] synthesized sericin-like proteins based on the Ser-rich repetitive motif and showed that the proteins self-assemble into fibrillar structures during dialysis as a formation of β-sheets. They speculated that polar zipper interactions through hydrogen bonding among abundant polar amino acids in the Ser-rich repetitive motif are responsible for fibril formation. Polar zipper interaction has been known to play a major role in assembling polar amyloidogenic peptide into fibrillar structure.[41,42] The experimental results obtained in this study suggest the contribution of polar zipper interactions to the aggregation of the repetitive regions in sericin molecules. Recently, self-complementing side-chain packing called steric zipper has been considered to be important factor in fibril formation of polar amyloidogenic peptides.[43−45] Asn and Gln have been often found to be involved in these polar zipper and steric zipper interactions. On the other hand, Ser has been often found to be involved in interhelical interaction called Ser zipper stabilizing transmembrane helices.[46,47] North and colleagues[47] revealed that efficient packing of relatively small Ser side chains contributed largely to the stabilization of transmembrane helices rather than hydrogen bonding. Therefore, the steric packing of the hydroxyl side chains might be an important factor to stabilize the aggregation of the β-sheets in sericin. More detailed investigations of sericin-derived peptide motifs would give us a new insight into protein aggregation.

Conclusions

The molecular mechanism behind the stabilization of the solid structure of sericin, a gluelike protein of *Bombyx mori* cocoon, was investigated by ^{13}C solid-state NMR spectroscopy. The CP/MAS and DD/MAS experiments of the native sericin derived from Sericin Hope silkworm have revealed that the hydroxyl side chains of the Ser and Thr residues in β-sheet structure remain rigid after hydration. This behavior was attributable to the Ser-rich repetitive region which covers large part of the primary structure of Ser1C, the main component of sericin. Site specific structural analysis using the ^{13}C-labeled model peptide indicated that the Ser and Thr linkage sequences such as SST, SSS, and SSTS form rigid and hydrophobic domains. It was speculated that the OH groups of the Ser and Thr side chains in β-sheet conformation interact with the adjacent sheets through hydrogen bonding to form the β-sheet aggregates. The formation and aggregation of β-sheets probably play a major role in stabilizing the solid structure of sericin and preventing it from dissolving in water. Moreover, controlling the manner of hydrogen bonding in sericin would lead to the production of sericin materials with improved material properties which are useful in biomedical fields.

Acknowledgment. We thank Dr. Keisuke Mase, National Institute of Agrobiological Sciences, for providing the eggs of Sericin Hope silkworm. We are grateful to Dr. Hajime Saito for his thorough reading of the manuscript. This work was partially supported by the Insect Technology Project from the Ministry of Agriculture, Forestry, and Fisheries of Japan.

References and Notes

(1) Drury, J. L.; Mooney, D. J. *Biomaterials* **2003**, *24*, 4337−4351.
(2) Kaplan, D. L. Silk. In *Protein-Based Materials*, McGrath, K., Kaplan, D., Eds.; Birkhauser: Boston, 1997; pp 103−131.
(3) Kameda, T.; Ohkawa, Y.; Yoshizawa, K.; Naito, J.; Ulrich, A. S.; Asakura, T. *Macromolecules* **1999**, *32*, 7166−7171.
(4) Yao, J.; Ohgo, K.; Sugino, R.; Kishore, R.; Asakura, T. *Biomacromolecules* **2004**, *5*, 1763−1769.
(5) White, J. L.; Wang, X. W. *Macromolecules* **2002**, *35*, 2633−2639.
(6) Fedic, R.; Zurovec, M.; Sehnal, F. *J. Insect Biotechnol. Sericol.* **2002**, *71*, 1−15.
(7) Craig, C. L.; Riekel, C. *Comp. Biochem. Physiol. B: Biochem. Mol. Biol.* **2002**, *133*, 493−507.
(8) Garel, A.; Deleage, G.; Prudhomme, J. C. *Insect Biochem. Mol. Biol.* **1997**, *27*, 469−477.
(9) Takasu, Y.; Yamada, H.; Tsubouchi, K. *Biosci. Biotechnol. Biochem.* **2002**, *66*, 2715−2718.
(10) Mase, K.; Iizuka, T.; Okada, E.; Miyajima, T.; Yamamoto, T. *J. Insect Biotechnol. Sericol.* **2006**, *75*, 85−88.
(11) Teramoto, H.; Kakazu, A.; Asakura, T. *Macromolecules* **2006**, *39*, 6−8.
(12) Teramoto, H.; Miyazawa, M. *J. Insect Biotechnol. Sericol.* **2003**, *72*, 157−162.
(13) Teramoto, H.; Miyazawa, M. *Biomacromolecules* **2005**, *6*, 2049−2057.
(14) Zhang, Y. Q. *Biotechnol. Adv.* **2002**, *20*, 91−100.
(15) Voegeli, R.; Meier, J.; Blust, R. *Cosmet. Toiletries* **1993**, *108*, 101−108.
(16) Takeuchi, A.; Ohtsuki, C.; Miyazaki, T.; Kamitakahara, M.; Ogata, S.; Yamazaki, M.; Furutani, Y.; Kinoshita, H.; Tanihara, M. *J. R. Soc. Interface* **2005**, *2*, 373−378.
(17) Takeuchi, A.; Ohtsuki, C.; Miyazaki, T.; Tanaka, H.; Yamazaki, M.; Tanihara, M. *J. Biomed. Mater. Res. A* **2003**, *65*, 283−289.
(18) Tsubouchi, K.; Igarashi, Y.; Takasu, Y.; Yamada, H. *Biosci. Biotechnol. Biochem.* **2005**, *69*, 403−405.
(19) Asakura, T.; Sugino, R.; Yao, J.; Takashima, H.; Kishore, R. *Biochemistry* **2002**, *41*, 4415−4424.
(20) Komatsu, K. *Bull. Seric. Exp. Stn.* **1969**, *23*, 499−514.
(21) Ishikawa, S.; Kurosu, H.; Ando, I. *J. Mol. Struct.* **1991**, *248*, 361−372.
(22) Kameda, T. *J. Phys. D: Appl. Phys.* **2005**, *38*, 4313−4320.
(23) Yang, Z.; Liivak, O.; Seidel, A.; LaVerde, G.; Zax, D. B.; Jelinski, L. W. *J. Am. Chem. Soc.* **2000**, *122*, 9019−9025.
(24) Holland, G. P.; Lewis, R. V.; Yarger, J. L. *J. Am. Chem. Soc.* **2004**, *126*, 5867−5872.
(25) Reichert, D.; Pascui, O.; deAzevedo, E. R.; Bonagamba, T. J.; Arnold, K.; Huster, D. *Magn. Reson. Chem.* **2004**, *42*, 276−284.
(26) Saito, H.; Yokoi, M. *J. Biochem. (Tokyo)* **1992**, *111*, 376−382.
(27) Lai, S.; Locci, E.; Saba, G.; Husu, I.; Masci, G.; Crescenzi, V.; Lai, A. *J. Polym. Sci., Part A: Polym. Chem.* **2003**, *41*, 3123−3131.
(28) Saito, H.; Ando, I. In *Annual Reports on NMR Spectroscopy*; Webb, G. A., Ed.; Academic Press: London, 1989; Vol. 22, pp 209−290.
(29) Ricciardi, R.; Gaillet, C.; Ducouret, G.; Lafuma, F.; Laupretre, F. *Polymer* **2003**, *44*, 3375−3380.
(30) Kobayashi, M.; Ando, I.; Ishii, T.; Amiya, S. *J. Mol. Struct.* **1998**, *440*, 155−164.
(31) Kobayashi, M.; Ando, I.; Ishii, T.; Amiya, S. *Macromolecules* **1995**, *28*, 6677−6679.
(32) Um, I. C.; Kweon, H. Y.; Lee, K. G.; Park, Y. H. *Int. J. Biol. Macromol.* **2003**, *33*, 203−213.
(33) Jackson, M.; Mantsch, H. H. *Crit. Rev. Biochem. Mol. Biol.* **1995**, *30*, 95−120.
(34) Komatsu, K. *Bull. Seric. Exp. Stn.* **1975**, *26*, 135−245.
(35) Zhu, L. J.; Arai, M.; Hirabayashi, K. *J. Seric. Sci. Jpn.* **1995**, *64*, 420−426.
(36) Klop, E. A.; Lammers, M. *Polymer* **1998**, *39*, 5987−5998.
(37) Okamoto, H.; Ishikawa, E.; Suzuki, Y. *J. Biol. Chem.* **1982**, *257*, 15192−15199.
(38) Michaille, J. J.; Garel, A.; Prudhomme, J. C. *Gene* **1990**, *86*, 177−184.
(39) Huang, J.; Valluzzi, R.; Bini, E.; Vernaglia, B.; Kaplan, D. L. *J. Biol. Chem.* **2003**, *278*, 46117−46123.
(40) Nakazawa, Y.; Asakura, T. *J. Am. Chem. Soc.* **2003**, *125*, 7230−7237.

(41) Perutz, M. F.; Johnson, T.; Suzuki, M.; Finch, J. T. *Proc. Natl. Acad. Sci. U.S.A.* **1994**, *91*, 5355−5358.
(42) Chan, J. C.; Oyler, N. A.; Yau, W. M.; Tycko, R. *Biochemistry* **2005**, *44*, 10669−10680.
(43) Nelson, R.; Sawaya, M. R.; Balbirnie, M.; Madsen, A. O.; Riekel, C.; Grothe, R.; Eisenberg, D. *Nature (London)* **2005**, *435*, 773−778.
(44) Zheng, J.; Ma, B.; Tsai, C.-J.; Nussinov, R. *Biophys. J.* **2006**, *91*, 824−833.
(45) Nelson, R.; Eisenberg, D. *Curr. Opin. Struct. Biol.* **2006**, *16*, 260−265.
(46) Adamian, L.; Liang, J. *Proteins* **2002**, *47*, 209−218.
(47) North, B.; Cristian, L.; Fu, Stowell, X.; Lear, J. D.; Saven, J. G.; Degrado, W. F. *J. Mol. Biol.* **2006**, *359*, 930−939.

MA062604E